

# Electrical stimulation of denervated rat skeletal muscle retards trabecular bone loss in early stages of disuse musculoskeletal atrophy

H. Tamaki<sup>1</sup>, K. Tomori<sup>2</sup>, K. Yotani<sup>3</sup>, F. Ogita<sup>3</sup>, K. Sugawara<sup>1</sup>, H. Kirimto<sup>1</sup>,  
H. Onishi<sup>1</sup>, N. Yamamoto<sup>1,4</sup>, N. Kasuga<sup>5</sup>

<sup>1</sup>Institute for Human Movement and Medical Sciences, Niigata University of Health and Welfare, Japan;  
<sup>2</sup>Kanagawa University of Human Services, Japan; <sup>3</sup>National Institute of Fitness and Sports in Kanoya, Japan;  
<sup>4</sup>Niigata Rehabilitation Hospital, Japan; <sup>5</sup>Department of Physical Education, Aichi University of Education, Japan

## Abstract

**Objectives:** We aimed to determine the intensity of muscle stimulation required to prevent structural failure as well as bone and skeletal muscle loss after denervation-induced disuse. **Methods:** Seven-week-old rats (weight, 198-225 g) were randomly assigned to age-matched groups comprising control (CON), sciatic nerve denervation (DN) or direct electrical stimulation (ES) one day later [after denervation] with 4, 8 and 16 mA at 10 Hz for 30 min/day, six days/week, for one or three weeks. Bone architecture and mean osteoid thickness in histologically stained tibial sections and tension in tibialis anterior muscles were assessed at one and three weeks after denervation. **Results:** Direct ES with 16 mA generated 23-30% maximal contraction force. Denervation significantly decreased trabecular bone volume fraction, thickness and number, connectivity density and increased trabecular separation in the DN group at weeks one and three. Osteoid thickness was significantly greater in the ES16 group at week one than in the DN and other ES groups. Trabecular bone volume significantly correlated with muscle weight. **Conclusions:** Relatively low-level muscle contraction induced by low-frequency, high-intensity electrical muscle stimulation delayed trabecular bone loss during the early stages (one week after DN) of musculoskeletal atrophy due to disuse.

**Keywords:** Electrical Stimulation, Muscle Force, Bone Volume, Disuse, Atrophy

## Introduction

Both the mass and structure of bone tissues adapt to the mechanical loading of gravity and movement. Limb disuse due to denervation causes musculoskeletal atrophy, together with changes in structural and functional profiles. We previously showed that trabecular bone loss and morphological changes due to denervation start during the first week after surgery and gradually decrease over the next three weeks<sup>1</sup>. Muscle mass also rap-

idly decreases during the first week after denervation to 50% of basal control levels<sup>2</sup>. Transcutaneous electrical stimulation (ES) is generally applied to patients undergoing physical rehabilitation to maintain and/or recover mass and force in denervated muscles. Some clinical reports have found that that direct ES to denervated muscles in patients with spinal cord injury (SCI) increases muscle mass and average fiber diameter<sup>3,4</sup>. Some findings of experimental animals lend further support to the notion that ES helps to limit denervation-induced muscle atrophy and improve muscle force and recovery<sup>5-7</sup>, whereas other studies have generated contradictory results<sup>8-10</sup>. Some studies have found that the effects of ES on muscle atrophy are influenced by the type of disuse models and the nature of experimental regimens such as the intensity, frequency and number of contractions<sup>11,12</sup>.

On the other hand, muscle contraction force confers mechanical load upon bone tissue. Some studies have demonstrated that even low-magnitude mechanical stimuli increase bone and muscle mass in studies of disused muscles in humans and other animals<sup>13-15</sup>. Therefore, ES-induced muscle contraction force

The authors have no conflict of interest.

Corresponding author: Hiroyuki Tamaki Ph.D., Institute for Human Movement and Medical Sciences, Niigata University of Health and Welfare, 1398 Shimami, Kita-ku, Niigata 950-3198, Japan  
E-mail: hiroyuki-tamaki@nuhw.ac.jp

Edited by: S. Warden  
Accepted 8 March 2014

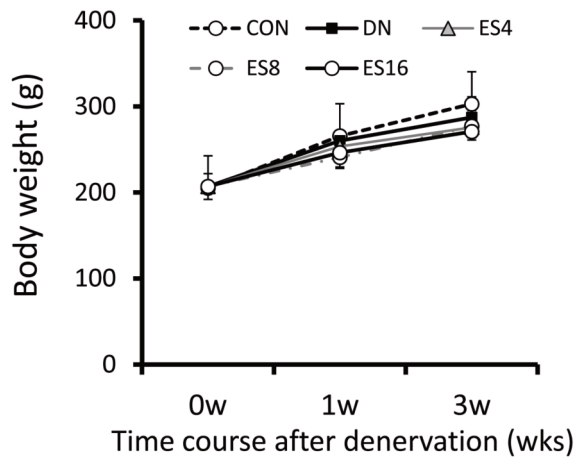


**Figure 1.** Time courses of body weight of control (CON), sciatic denervation (DN) and DN with electric stimulation (ES4, ES8 and ES16) groups.

would help to prevent/reduce disuse-induced osteopenia because mechanical loading is a major influence on bone volume and architecture<sup>16,17</sup>. Osteopenia of the distal femur and proximal tibia and the loss of quadriceps strength in humans with SCI can be partly reversed by training assisted by ES at 25 Hz for 24 weeks<sup>18</sup>. Dynamic muscle stimulation with mid-, and high-frequency ES (>20 Hz) inhibited trabecular bone loss of the femur in a suspension disuse model for four weeks<sup>19</sup>. Such stimulation with 10 Hz was not examined in that study. The notion that a higher ES frequency increases muscle contraction force is conceivable because of the summation of twitch contraction<sup>20</sup>. Qin et al. reported that electrical muscle stimulation between 1 and 100 Hz might generate nonlinear bone stress and fluid pressure in bone, and that 10 Hz produces maximal strain on bone, which helps to mitigate bone loss<sup>21,22</sup>. On the other hand, electrical muscle stimulation at a cycling rate might generate muscle mass but it is not necessary to prevent bone loss<sup>23</sup>. It would be important to explore the potential of muscle stimulation with 10 Hz should be explored from the viewpoint of reducing the volume of disused muscle and bone loss.

Skeletal muscle is also a resource for generating force. An ES training regimen that would reduce structural and functional damage in denervated muscle fibers might potentiate the anabolic activity of bone tissue through mechanical loads on bone induced by muscle force. We previously assessed the appropriate stimulation intensity according to individual structural recovery of skeletal muscle after denervation and found that high-intensity (16 mA) ES retarded denervated muscle atrophy and up-regulated the expression of insulin-like growth factor-1 (IGF-1) mRNA<sup>24</sup>. However, this intensity of ES might adversely affect the regeneration of nerve terminals and/or the membrane systems involved in excitation-contraction (e-c) coupling which is the physiological process of converting an electrical stimulus to the mechanical activation of the contractile myofibrils. Conversely, middle- and low-intensity (4 and 8 mA) ES regenerated mem-

brane systems involved in e-c coupling and nerve terminals, but did not retard denervated muscle atrophy. This dilemma indicates the importance of establishing the appropriate stimulation intensity according to the individual structural and functional profiles that are targeted for improvement. Similarly, whether the ES regimen can prevent/reduce muscle and bone loss induced by disuse is important for the development of clinical interventions.

Here, we assessed effective stimulation intensity according to the prevention of individual structural failure and loss of bone and skeletal muscle after inducing disuse by denervation. We thus applied direct ES at three intensities of current to denervated rat tibialis anterior (TA) muscles. We confirmed the muscle force induced at these intensities and assessed the effects of ES on the atrophy process in terms of the volume and architectural profiles of trabecular bone and muscle mass at one and three weeks after denervation.

## Materials and methods

### Animals and denervation

Eighty-six male Wistar rats (CLEA, Tokyo, Japan) were individually housed in standard cages under a constant temperature ( $23\pm 2^\circ\text{C}$ ), humidity ( $55\pm 5\%$ ), and 12-h:12-h light-dark cycles, and provided with CE-2 rodent chow (CLEA) and water *ad libitum*. When they reached seven weeks of age (body weight, 198–225 g), the rats were randomly assigned to the following groups: age-matched controls (CON,  $n=15$ ), and denervation without (DN,  $n=15$ ), or with direct electrical stimulation (ES,  $n=44$ ). The ES group was subdivided into groups that were stimulated with 4 (ES4,  $n=15$ ), 8 (ES8,  $n=15$ ), and 16 (ES16,  $n=14$ ) mA. Basal control rats ( $n=12$ ) were sacrificed at seven weeks of age. Tibiae and TA muscles were collected from the basal group and from the CON, DN and ES groups at one and three weeks after denervation. The rats in the DN and ES groups were anesthetized with an intraperitoneal injection of sodium pentobarbital (40 mg/kg body weight). The skin covering the buttock was cut on the left side, and the sciatic nerve was exposed and separated from the surrounding tissue. The sciatic nerve was frozen for 5 s with a stainless steel rod (5 mm diameter) that had been cooled in liquid nitrogen<sup>1,25,26</sup>. This freezing procedure uniformly damages nerve fibers, although they are more likely to become re-innervated using this procedure compared to others, such as nerve crushing, cutting or transection with a suture<sup>24-26</sup>. Neurectomy creates an enduring model of leg disuse for situations where subsequent natural recovery is not desired. However, freezing nerves creates a model of temporary disuse that allows complete immobilization of innervated muscles for a specific period by temporarily disabling peripheral nerve function, thus allowing observation of the post-atrophy recovery process. We previously reported that tibial bone loss continues for three weeks and recovers for ten weeks after freezing the nerve<sup>1</sup>. All animal manipulations and protocols proceeded in accordance with the guidelines presented in the Guiding Principles for the Care and Use of Animals in the Field of Physiological Sciences, published by the Physiological Society of Japan. This study was approved by the Animal Committee of the National Institute of Fitness and Sports.

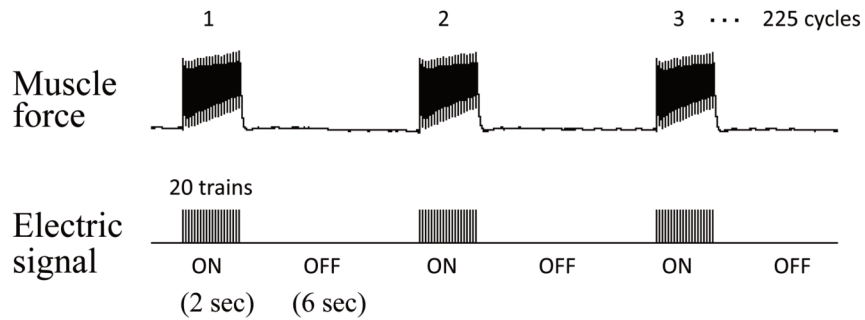


**Figure 2.** Representative muscle force profile induced by muscle stimulation at 10 Hz. Electric stimulation (ES) at 10 Hz was applied for 2 sec followed by 6 sec of rest and repeated for 225 cycles in total. This level of ES caused little summation of twitch contraction.

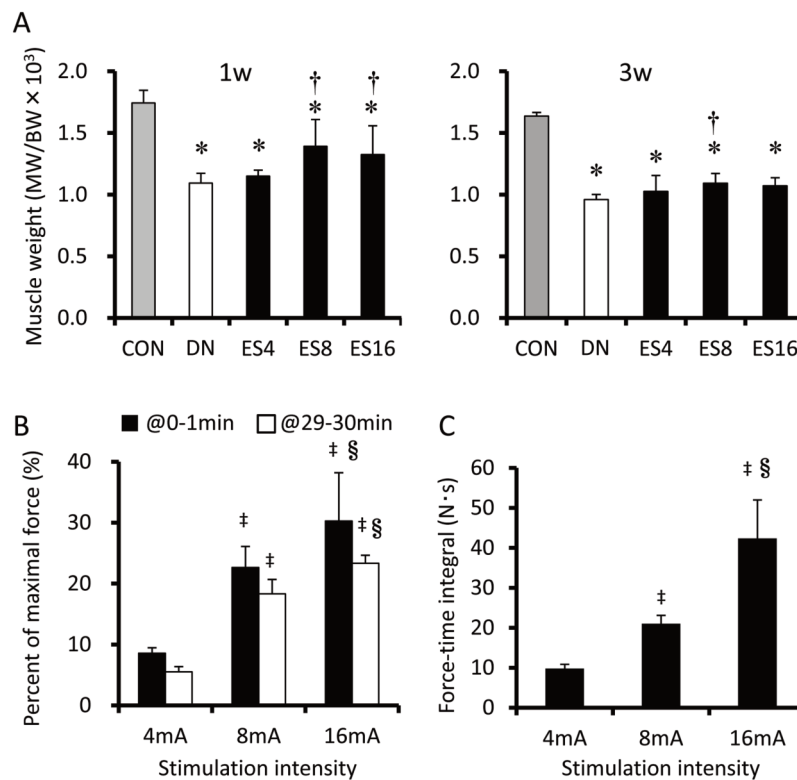


**Figure 3.** Relative weight of tibialis anterior muscle at one (1w) and three (3w) weeks after denervation (A) and ratio (%) of tibialis anterior (TA) muscle force relative to maximal tetanic force (B) and force-time integral (C) induced by electrical stimulation at intensities of 4, 8 and 16 mA at 10Hz. Electric stimulation (ES) at 16 mA elicited the highest values among three intensities. CON, age-matched control; DN, denervation without ES; ES4, ES8 and ES16, denervation with ES at 4, 8, and 16 mA, respectively. \* $P < 0.05$  vs. CON; † $P < 0.05$  vs. DN. Values are means  $\pm$  SD. ‡ $P < 0.05$  vs. 4 mA; § $P < 0.05$  vs. 8 mA.

*Direct ES procedures*

The day after muscle denervation, the TA muscle in all ES groups were electrically stimulated by ES using Torio300 and SEM-4201 electrostimulators (Sakai, Tokyo, Japan and Nihon Kohden, Tokyo, Japan, respectively) with an isolator, and paired silver surface electrodes (diameter 3 mm). The age-matched control, DN and ES groups were anesthetized by

isoflurane inhalation (1.5-2.5%), and surface electrodes were attached to the shaved anterior surface of the left leg only in the ES rats. The left TA muscle was stimulated with an intensity of 4, 8 or 16 mA at a frequency of 10 Hz and pulse width of 250  $\mu$ s, for 30 min per day, six days per week, for one or three weeks. The ES regimen comprised two seconds of stimulation followed by six seconds of rest (Figure 2). Age-

matched control and DN rats were also anesthetized for the same duration as the ES group. Although the individual ES regimen did not cause maximal contraction (10-30% maximal contraction force; Figure 3) in denervated TA muscle, toe flexion was visible.

#### *Electrical stimulation evoked muscle contraction force*

We measured TA muscle tension under the described stimulus conditions to determine which mechanical factors are evoked by direct ES at various intensities<sup>26</sup>. Briefly, seven-week-old rats (n=8) were anesthetized by continuous isoflurane inhalation and placed on a heated plate to maintain body temperature. The lower limb was secured and stabilized on the working platform with restraining bars and pins at the knee and ankle joints. The distal tendon of the TA was oriented along the natural pull of the muscle and attached to a TB-654T isometric transducer (Nihon Kohden)<sup>27</sup> that was secured with a 4-0 silk suture on a three-dimensional drive precision stage<sup>28</sup>. A pair of silver electrodes (diameter 3 mm) was mounted on the TA muscle, which was connected to electrostimulators. Isometric contraction force and force-time integrals were measured under the same stimulation conditions with the daily direct ES regimen. Maximum tetanic force was also determined from the average of three tetani. The muscle tension signal was sampled at 2 kHz through a PowerLab 8SP A/D converter (ADInstruments, Nagoya, Japan).

#### *Tissue sampling*

The TA muscles were harvested from rats anesthetized with sodium pentobarbital (40 mg/kg body weight), weighed at the end of the experiment and then TA muscle weight (MW) was normalized by body weight (BW) and is expressed as a ratio of MW/BW. A mixed fixative (0.1 mol/L sodium cacodylate buffer pH 7.35 containing 1% glutaraldehyde, 1% formaldehyde and 0.05% CaCl<sub>2</sub>) was injected via the abdominal aorta and perfusion fixation proceeded at room temperature for 30 min. The tibiae were removed and preserved in 70% ethanol.

#### *Microcomputed tomography ( $\mu$ CT)*

Tibial bone microarchitecture was measured using a SkyScan 1076 high-resolution micro CT scanner (SkyScan, Kontich, Belgium). The specimens were wrapped in plastic film to prevent drying while acquiring images under the following conditions: source voltage, 70 kV; current, 141  $\mu$ A; rotation step, 0.6°; full rotation >180°; aluminium filter (to reduce beam hardening), 1 mm; pixel size, 17.67  $\mu$ m, exposure, 0.54 seconds. Three-dimensional (3D) microstructural image data were reconstructed using NRecon software (SkyScan). Morphometric parameters were calculated using CT Analyzer (CTAn) software (SkyScan) for trabecular bone in the tibiae. Trabecular bone within the proximal tibiae was extracted by semi-automatically drawing interactive polygons on two-dimensional (2D) sections. The volume of interest (VOI) started at a distance of 1 mm from the lower end of the growth plate and extended distally for 113 cross sections (height, 2 mm). The VOI comprised only trabecular bone and the marrow cav-

ity. The following parameters were measured according to the guidelines for assessing bone microstructure in rodents using micro CT<sup>29</sup>: bone volume fraction (BV/TV, %), trabecular number (Tb.N), trabecular thickness (Tb.Th), trabecular spacing (Tb.Sp), and connection density (Conn.D).

#### *Bone histological staining*

After micro CT imaging, each tibia was cut sagittally at the proximal end and decalcified in 0.1 mol/L EDTA (pH 7.35) at 4°C for 2-3 weeks and embedded in paraffin. Longitudinal sections (5- $\mu$ m thick) were stained with hematoxylin and eosin (H-E) or Azan. Osteoid in decalcified specimens was stained with H-E using the Golland-Yoshiki method<sup>30</sup> as described<sup>1</sup>. We measured at least 15 regions per field at 400-fold magnification to calculate mean osteoid thickness (O.Th)<sup>31</sup> using a light/fluorescence microscope (BX61, Olympus, Tokyo, Japan) and Image-Pro Plus 5 image analysis software (Media Cybernetics, Rockville, MD, USA).

#### *Statistical analysis*

All data are expressed as means  $\pm$  standard deviation. Kruskal-Wallis analysis of variance on ranks followed by the Dunn's multiple test was applied to assess the statistical significance of differences among the groups. Mean values in trabecular bone volume (BV/TV) and muscle weight (MW/BW) in each group at each time point were normalized as ratios (%) relative to basal control group value. The relationship between mean %BV/TV and muscle weight was determined using Pearson's correlation coefficient. Significance levels were set at  $P < 0.05$ .

## **Results**

#### *Body weight*

Figure 1 shows that all rats gained a significant amount of weight during the experimental period ( $P < 0.05$ ). Body weight did not significantly differ among the groups at one week after denervation. The ES and DN groups weighed 5.2-10.6% less than the age-matched control group at three weeks after denervation ( $P < 0.05$ ), but the ES and DN groups did not significantly differ.

#### *Muscle weight and ES evoked muscle contraction force*

The weight of the TA muscle relative to body weight (MW/BW) significantly decreased after denervation ( $P < 0.05$ ), and the CON and DN groups significantly differed. Muscle weight did not recover to either the basal level or the level of the age-matched control group after ES for one or three weeks (Figure 3A). However, the relative muscle weight was significantly higher in both the ES8 and ES16 groups than in the DN group at week one only ( $P < 0.05$ ). Direct ES at 10 Hz evoked significantly more muscle contraction force in the TA with stimulation intensity at both the beginning (0-1 min period) and the end (29-30 min period) of ES for 30 min (Figure 3B). Direct ES with 16 mA generated 23-30% of the maximal contraction force. Force-time integrals evoked by ES of 16 mA were the highest among the three stimulation intensities (Figure 3C).

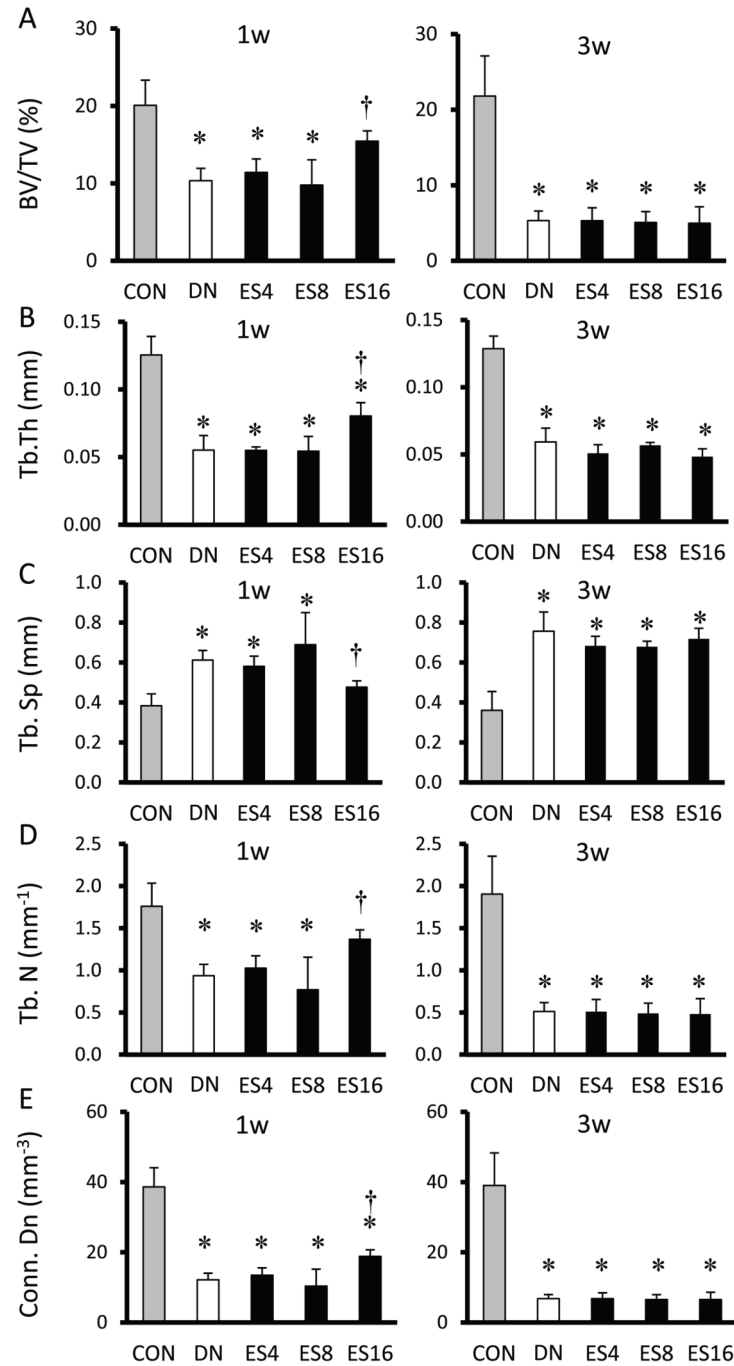


**Figure 4.** Trabecular bone volume and microarchitectural parameters of tibiae at one (1w) and three (3w) weeks after denervation. BV/TV, trabecular bone volume fraction (A); Tb.Th, trabecular thickness (B); Tb.Sp, trabecular separation (C); Tb.N, trabecular number (D); Conn.D, connectivity density (E); CON, age-matched control; DN, denervation without ES; ES4, ES8 and ES16, denervation with ES at 4, 8 and 16 mA, respectively. \* $P < 0.05$  vs. CON; † $P < 0.05$  vs. DN. Values are means  $\pm$  SD.

### Bone analysis

Denervation resulted in significantly less trabecular bone volume fraction (BV/TV), trabecular thickness (Tb.Th), trabecular number (Tb.N), connectivity density (Conn.D) and increased trabecular separation (Tb.Sp) in the DN, than in the CON group

in weeks one and three ( $P < 0.05$ ; Figure 4A-E). These values did not recover to the control level after ES for one or three weeks. However, these parameters were significantly higher in the ES16, than in the DN group at week one ( $P < 0.05$ ). Regarding the time course of BV/TV relative to the basal control after DN,

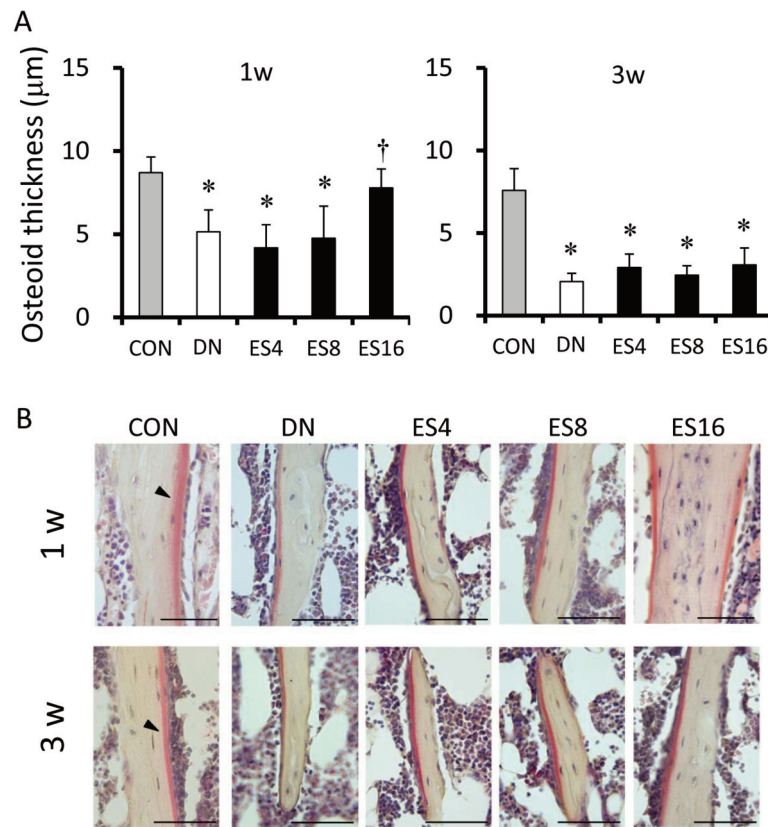


**Figure 5.** Histomorphometric findings of osteoid thickness and light microscopy of osteoid matrix at trabecular bone. (A) Histomorphometric findings of mean osteoid thickness at one (1w) and three (3w) weeks after DN with or without ES. (B) Micrographs show distinct eosinophilia of osteoid matrix (arrowhead) at trabecular bone stained with hematoxylin and eosin. CON, age-matched control (100% at 0w); DN, denervation group without ES; ES4, ES8 and ES16, denervation with ES at 4, 8 and 16 mA, respectively. Bar=50 µm. \* $P < 0.05$  vs. CON; † $P < 0.05$  vs. DN. Values are means  $\pm$  SD.

the process of BV/TV loss was more gradual in the ES16, than in the other ES and DN groups. The BV/TV was significantly higher in the CON, than in the ES4, ES8 and DN ( $P < 0.05$ ), but not the ES16 group at week one. Osteoid thickness was also significantly lower in the DN and ES, than in the CON group ( $P < 0.05$ ), except for the ES16 group at week one (Figure 5). Osteoid thickness at week one was significantly greater in the ES16, than in the DN ( $P < 0.05$ ), but not the ES4 and ES8 groups.

#### Muscle weight and bone volume correlation

Correlations between ratios (%) of changes in trabecular bone volume (BV/TV) and muscle weight (MW/BW) relative to basal-control levels were analyzed at each time point after DN in each group (Figure 6). The correlation between BV/TV and muscle weight was significant ( $P < 0.0001$ ), with a correlation coefficient of 0.94.

## Discussion

The present findings showed that electrical stimulation-induced muscle force could decrease denervation-induced os-

teopenia at the early stage of disuse atrophy. The ability of the relatively highest ES (ES16) to reduce bone loss, trabecular architecture deterioration and osteoid formation was accompanied by the attenuation of muscle atrophy. In addition, the % reduction in trabecular bone volume closely correlated with muscle weight at after three weeks of ES to treat DN.

Frequency-dependent muscle stimulation (20-100 Hz) for four weeks inhibited trabecular bone loss in the disused rat femur<sup>19</sup>. A higher ES frequency under these conditions would cause higher muscle contraction force because of the summation of twitch contraction and result in higher force-time integrals during ES intervention. We applied stimulation intensities of 4, 8 and 16 mA at 10 Hz. The ES at an intensity of 16 mA and a frequency of 10 Hz, caused little summation of twitch contraction, and elicited about 30% of maximal muscle contraction force in the TA. These results showed that ES at 16 mA reduced trabecular bone loss and structural changes in the tibia after one week of denervation with ES, whereas ES at 4 and 8 mA did not. However, ES did not reduce trabecular bone loss at all stimulation intensities at three weeks of denervation with ES. Our data indicated that relatively high-inten-

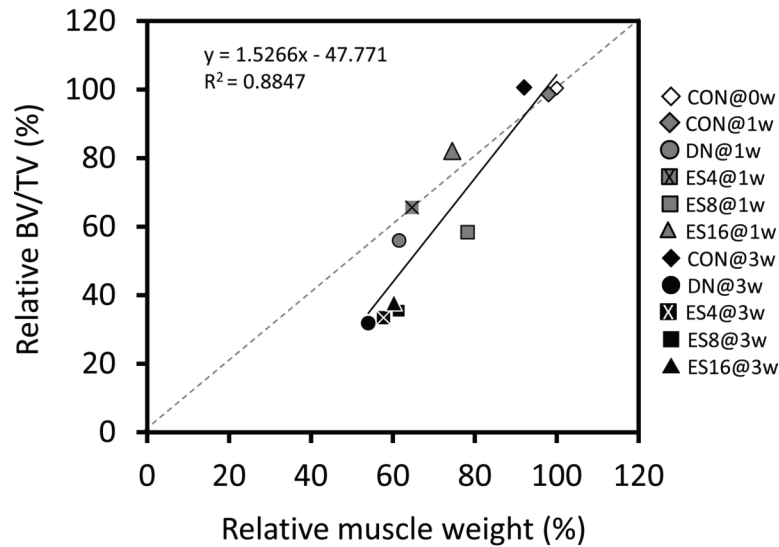


**Figure 6.** Correlations between muscle weight (MW/BW) and bone volume fraction (BV/TV) relative to basal-control values (100%) after DN with or without ES.

sity (16 mA) ES, which does not cause tetanic muscle contraction, would retard trabecular bone loss and structural changes at the early stages of disuse atrophy.

We previously reported that high-intensity (16 mA) ES retarded denervated muscle atrophy, although it might adversely affect the regeneration of nerve terminals and/or the membrane systems involved in e-c coupling after three weeks of denervation<sup>24</sup>. We speculated that muscle denervation for three weeks with ES (16 mA) in the present study could not provide sufficient functional load to reduce bone loss and that the appropriate intensities should be determined to generate a reduction in structural and functional damage in denervated muscle fibers.

The relative muscle weight was significantly higher in the ES8 and ES16, than in the DN group. However, muscle weight in all DN and ES groups gradually decreased over three weeks. Muscle weight was 21% and 11% higher in the ES16, than in the DN group after one and three weeks of ES, respectively. Electrical stimulation reduced muscle atrophy after DN more effectively at one, than at three weeks. A decrease in muscle mass as a force-generating resource would result in a decrease in mechanical stress to bone during ES. Although we did not determine mechanical strain in the tibia during daily ES intervention, the magnitude of mechanical strain induced by direct ES in the tibia might be lower at three weeks than at one week after DN. This might be one reason why ES did not reduce trabecular bone loss after DN at three weeks. Moreover, osteoid was significantly thicker in the ES16 than the other ES groups at one, but not at three weeks. This suggests that osteoblasts maintained more bone collagen formation in the ES16 group for one week after DN with ES. Therefore, the maintained osteoid formation appeared to reflect retardation of the decrease in trabecular bone thickness at one week after DN.

We also found a significantly close correlation coefficient

between relative BV/TB fractions and relative muscle weight under our experimental conditions. This indicates that maintaining muscle mass after DN with or without ES appreciably impacts trabecular bone loss, and an ES regimen that can prevent/retard muscle atrophy and maintain a muscle force output sufficient to exert mechanical stress on bone tissue should be important.

The effects of ES on the reduction of bone loss due to disuse might be explained by the induction of mechanical and humoral factors by muscle contraction and ES. Although we did not examine bone strain in the present study, mechanical loading is a major functional influence on the mass and structure of bone tissue. The adaptive response of bone to mechanical loading is essentially linear between peak dynamic load and changes that occur in trabecular bone after denervation<sup>17</sup>. Even low-magnitude mechanical stimuli (<10 microstrains) increase bone formation in animal models of disuse<sup>15,32</sup>. Mechanotransduction converts physical forces into biochemical signals that are then integrated into cellular responses<sup>33</sup>. During mechanical signal transmission, osteoblasts, osteocytes and cells that line bone might act as sensors. These cells also produce growth factors that might signal osteoprogenitors to differentiate into osteoblasts and promote osteoblast activity<sup>34</sup>. Mechanical loading promotes bone formation<sup>35</sup>, osteoblastic differentiation and activity, and lining-cell reactivation<sup>36</sup>, while inhibiting the expression of osteoclast differentiation factor and osteoclast numbers<sup>37</sup>. Mechanical stimuli of osteoblasts also induce the secretion of growth factors including insulin-like growth factor (IGF), vascular endothelial growth factor (VGEF), transforming growth factor (TGF)- $\beta$ , and the bone morphogenetic protein (BMP) that are considered to be the principal local regulators of osteogenesis<sup>38</sup>.

Systemic effects of ES were not investigated in the present

study, but electrically stimulated muscle contraction enhances venous and arterial blood flow<sup>39</sup>, which subsequently increases intramedullary pressure (ImP) and fluid flow in bone<sup>40</sup>. Oscillatory fluid flow-induced shear stress decreases osteoclastogenesis<sup>41</sup> and stimulates osteoblast proliferation and differentiation<sup>42</sup>. The role of muscle-derived growth factors in bone formation has recently been discussed<sup>43,44</sup>. Muscle seems to be an important, local source of growth factors for bone tissue, yet the cellular and molecular mechanisms linking muscle and bone tissues are not well understood. Exercise and muscle contraction alter the secretion of several myokines that appear to affect bone metabolism<sup>44</sup>. Some authors have reported that myostatin (growth differentiation factor (GDF)-8) secretion in muscle inhibits bone formation<sup>45</sup>, whereas IGF-1 and fibroblast growth factor (FGF)-2 stimulate bone formation *in vivo* and *in vitro*<sup>46,47</sup>. Myokine secretion induced by muscle contraction might be one pathway of stimulating bone formation.

One limitation of this study is that we did not determine parameters of possible mechanisms that might explain the effects of ES on the reduction of bone loss due to disuse, and thus more studies are required to elucidate such mechanisms. Although dynamic and static histomorphometry analyses would increase understanding of bone formation and bone resorption, the main objective of this study was to assess the stimulation intensity required to prevent structural failure and loss of individual bone and skeletal muscle after disuse induced by denervation. Our data suggested that relatively small muscle contraction induced by low-frequency (10 Hz) high-intensity (16 mA) electrical muscle stimulation could delay trabecular bone loss during the early stages (only at week one after denervation) of musculoskeletal atrophy due to disuse.

#### Acknowledgements

This study was supported in part by a Grant-in-Aid for Scientific Research from the Japan Society for the Promotion of Science (project nos. C, 25350829 and B, 25282163), and by a Grant-in-Aid for Developed Research (B) from the Niigata University of Health and Welfare. The authors are grateful to the Niigata Bone Science Institute for technical support with the histomorphometry.

#### References

1. Tamaki H, Yotani K, Ogita F, Takahashi H, Kirimoto H, Onishi H, Yamamoto N. Changes over time in structural plasticity of trabecular bone in rat tibiae immobilized by reversible sciatic denervation. *J Musculoskelet Neuronal Interact* 2013;13:251-8.
2. Takekura H, Kasuga N, Kitada K, Yoshioka T. Morphological changes in the triads and sarcoplasmic reticulum of rat slow and fast muscle fibres following denervation and immobilization. *J Muscle Res Cell Motil* 1996; 17:391-400.
3. Kern H, Salmons S, Mayr W, Rossini K, Carraro U. Recovery of long-term denervated human muscles induced by electrical stimulation. *Muscle Nerve* 2005;31:98-101.
4. Modlin M, Forstner C, Hofer C, Mayr W, Richter W, Carraro U, Protasi F, Kern H. Electrical stimulation of denervated muscles: first results of a clinical study. *Artif Organs* 2005;29:203-6.
5. Guo BS, Cheung KK, Yeung SS, Zhang BT, Yeung EW. Electrical stimulation influences satellite cell proliferation and apoptosis in unloading-induced muscle atrophy in mice. *PLoS One* 2012;7:e30348.
6. Zhang BT, Yeung SS, Liu Y, Wang HH, Wan YM, Ling SK, Zhang HY, Li YH, Yeung EW. The effects of low frequency electrical stimulation on satellite cell activity in rat skeletal muscle during hindlimb suspension. *BMC Cell Biol* 2010;11:87.
7. Willand MP, Holmes M, Bain JR, Fahnstock M, De Bruin H. Electrical muscle stimulation after immediate nerve repair reduces muscle atrophy without affecting reinnervation. *Muscle Nerve* 2013;48:219-25.
8. Dow DE, Carlson BM, Hassett CA, Dennis RG, Faulkner JA. Electrical stimulation of denervated muscles of rats maintains mass and force, but not recovery following grafting. *Restor Neurol Neurosci* 2006;24:41-54.
9. Dow DE, Cederna PS, Hassett CA, Dennis RG, Faulkner JA. Electrical stimulation prior to delayed reinnervation does not enhance recovery in muscles of rats. *Restor Neurol Neurosci* 2007;25:601-10.
10. Gigo-Benato D, Russo TL, Geuna S, Domingues NR, Salvini TF, Parizotto NA. Electrical stimulation impairs early functional recovery and accentuates skeletal muscle atrophy after sciatic nerve crush injury in rats. *Muscle Nerve* 2010;41:685-93.
11. Dupont Salter AC, Richmond FJ, Loeb GE. Effects of muscle immobilization at different lengths on tetrodotoxin-induced disuse atrophy. *IEEE Trans Neural Syst Rehabil Eng* 2003;11:209-17.
12. Fujita N, Murakami S, Arakawa T, Miki A, Fujino H. The combined effect of electrical stimulation and resistance isometric contraction on muscle atrophy in rat tibialis anterior muscle. *Bosn J Basic Med Sci* 2011;11:74-9.
13. Gilsanz V, Wren TA, Sanchez M, Dorey F, Judex S, Rubin C. Low-level, high-frequency mechanical signals enhance musculoskeletal development of young women with low BMD. *J Bone Miner Res* 2006;21:1464-74.
14. Hannan MT, Cheng DM, Green E, Swift C, Rubin CT, Kiel DP. Establishing the compliance in elderly women for use of a low level mechanical stress device in a clinical osteoporosis study. *Osteoporos Int* 2004;15:918-26.
15. Rubin C, Xu G, Judex S. The anabolic activity of bone tissue, suppressed by disuse, is normalized by brief exposure to extremely low-magnitude mechanical stimuli. *FASEB J* 2001;15:2225-9.
16. Frost HM. Bone "mass" and the "mechanostat": a proposal. *Anat Rec* 1987;219:1-9.
17. Sugiyama T, Meakin LB, Browne WJ, Galea GL, Price JS, Lanyon LE. Bones' adaptive response to mechanical loading is essentially linear between the low strains associated with disuse and the high strains associated with the

- lamellar/woven bone transition. *J Bone Miner Res* 2012; 27:1784-93.
18. Belanger M, Stein RB, Wheeler GD, Gordon T, Leduc B. Electrical stimulation: can it increase muscle strength and reverse osteopenia in spinal cord injured individuals? *Arch Phys Med Rehabil* 2000;81:1090-8.
  19. Lam H, Qin YX. The effects of frequency-dependent dynamic muscle stimulation on inhibition of trabecular bone loss in a disuse model. *Bone* 2008;43:1093-100.
  20. Lieber RL. Skeletal muscle structure, function & plasticity: the physiological basis of rehabilitation. 2nd ed. Philadelphia: Lippincott Williams & Wilkins; 2002.
  21. Qin YX, Lam H. Intramedullary pressure and matrix strain induced by oscillatory skeletal muscle stimulation and its potential in adaptation. *J Biomech* 2009;42:140-5.
  22. Qin YX, Lam H, Ferreri S, Rubin C. Dynamic skeletal muscle stimulation and its potential in bone adaptation. *J Musculoskelet Neuronal Interact* 2010;10:12-24.
  23. Giangregorio L, McCartney N. Bone loss and muscle atrophy in spinal cord injury: epidemiology, fracture prediction, and rehabilitation strategies. *J Spinal Cord Med* 2006;29:489-500.
  24. Tomori K, Ohta Y, Nishizawa T, Tamaki H, Takekura H. Low-intensity electrical stimulation ameliorates disruption of transverse tubules and neuromuscular junctional architecture in denervated rat skeletal muscle fibers. *J Muscle Res Cell Motil* 2010;31:195-205.
  25. Sakakima H, Kawamata S, Kai S, Ozawa J, Matsuura N. Effects of short-term denervation and subsequent reinnervation on motor endplates and the soleus muscle in the rat. *Arch Histol Cytol* 2000;63:495-506.
  26. Takekura H, Tamaki H, Nishizawa T, Kasuga N. Plasticity of the transverse tubules following denervation and subsequent reinnervation in rat slow and fast muscle fibres. *J Muscle Res Cell Motil* 2003;24:439-51.
  27. Tamaki H, Murata F, Takekura H. Histomorphological evidence of muscle tissue damage and recording area using coiled and straight intramuscular wire electrodes. *Eur J Appl Physiol* 2006;98:323-7.
  28. Tamaki H, Yotani K, Yuki A, Kirimoto H, Sugawara K, Onishi H. Magnetic field strength properties in bone marrow during pulsed electromagnetic stimulation. *Journal of Biomedical Science and Engineering* 2010;3:1156-60.
  29. Bouxsein ML, Boyd SK, Christiansen BA, Guldberg RE, Jepsen KJ, Muller R. Guidelines for assessment of bone microstructure in rodents using micro-computed tomography. *J Bone Miner Res* 2010;25:1468-86.
  30. Yoshiki S. A simple histological method for identification of osteoid matrix in decalcified bone. *Stain Technol* 1973; 48:233-8.
  31. Fujimoto R, Tanizawa T, Nishida S, Yamamoto N, Soshi S, Endo N, Takahashi HE. Local effects of transforming growth factor-beta1 on rat calvaria: changes depending on the dose and the injection site. *J Bone Miner Metab* 1999;17:11-7.
  32. Rubin C, Turner AS, Bain S, Mallinckrodt C, McLeod K. Anabolism. Low mechanical signals strengthen long bones. *Nature* 2001;412:603-4.
  33. Huang C, Ogawa R. Mechanotransduction in bone repair and regeneration. *FASEB J* 2010;24:3625-32.
  34. Duncan RL, Turner CH. Mechanotransduction and the functional response of bone to mechanical strain. *Calcif Tissue Int* 1995;57:344-58.
  35. De Souza RL, Matsuura M, Eckstein F, Rawlinson SC, Lanyon LE, Pitsillides AA. Non-invasive axial loading of mouse tibiae increases cortical bone formation and modifies trabecular organization: a new model to study cortical and cancellous compartments in a single loaded element. *Bone* 2005;37:810-8.
  36. Chow JW, Wilson AJ, Chambers TJ, Fox SW. Mechanical loading stimulates bone formation by reactivation of bone lining cells in 13-week-old rats. *J Bone Miner Res* 1998; 13:1760-7.
  37. Rubin J, Murphy T, Nanes MS, Fan X. Mechanical strain inhibits expression of osteoclast differentiation factor by murine stromal cells. *Am J Physiol Cell Physiol* 2000; 278:C1126-32.
  38. Papachroni KK, Karatzas DN, Papavassiliou KA, Basdra EK, Papavassiliou AG. Mechanotransduction in osteoblast regulation and bone disease. *Trends Mol Med* 2009;15:208-16.
  39. Valic Z, Buckwalter JB, Clifford PS. Muscle blood flow response to contraction: influence of venous pressure. *J Appl Physiol* (1985) 2005;98:72-6.
  40. Qin YX, Lin W, Rubin C. The pathway of bone fluid flow as defined by *in vivo* intramedullary pressure and streaming potential measurements. *Ann Biomed Eng* 2002; 30:693-702.
  41. Kim CH, You L, Yellowley CE, Jacobs CR. Oscillatory fluid flow-induced shear stress decreases osteoclastogenesis through RANKL and OPG signaling. *Bone* 2006; 39:1043-7.
  42. Kapur S, Baylink DJ, Lau KH. Fluid flow shear stress stimulates human osteoblast proliferation and differentiation through multiple interacting and competing signal transduction pathways. *Bone* 2003;32:241-51.
  43. Hamrick MW, McNeil PL, Patterson SL. Role of muscle-derived growth factors in bone formation. *J Musculoskelet Neuronal Interact* 2010;10:64-70.
  44. Hamrick MW. A role for myokines in muscle-bone interactions. *Exerc Sport Sci Rev* 2011;39:43-7.
  45. Elkasrawy MN, Hamrick MW. Myostatin (GDF-8) as a key factor linking muscle mass and bone structure. *J Musculoskelet Neuronal Interact* 2010;10:56-63.
  46. Yakar S, Rosen CJ, Beamer WG, Ackert-Bicknell CL, Wu Y, Liu JL, Ooi GT, Setser J, Frystyk J, Boisclair YR, LeRoith D. Circulating levels of IGF-1 directly regulate bone growth and density. *J Clin Invest* 2002;110:771-81.
  47. Liang H, Pun S, Wronski TJ. Bone anabolic effects of basic fibroblast growth factor in ovariectomized rats. *Endocrinology* 1999;140:5780-8.